Available online at www.sciencedirect.com
ScienceDirect
Journal of Photochemistry and Photobiology A: Chemistry 186 (2007) 173–177
Journal of Photochemistry and Photobiology A:Chemistry
www.elsevier.com/locate/jphotochem

Photochromic response of nanoparticles of spiropyran–$MnPS_3$ intercalate: A search for optically bistable nanocomponents

Huijun Zhang [a], Tao Yi [a,*], Fuyou Li [a], Emilie Delahaye [b], Pei Yu [b], Rene Clement [b,**]

[a] *Department of Chemistry, Laboratory of Advanced Materials, Fudan University, 220 Handan Road, Shanghai 200433, China*
[b] *Laboratoire de Chimie Inorganique, U.M.R. 8613, Bat 420, Université Paris XI, 91405 Orsay, France*

Received 14 March 2006; received in revised form 31 July 2006; accepted 12 August 2006
Available online 22 August 2006

Abstract

Air-stable hybrid organic-inorganic nanoparticles comprising photochromic spiropyran (SP) species intercalated in layered $MnPS_3$ were prepared by a microemulsion procedure in cyclohexane, using Brij-97 (polyoxyethylene-oleyl ether) surfactant. The nanoparticles (10–20 nm in size) were precipitated, purified and redispersed in water or organic solvents. Thin films of the nanoparticles were casted from organic solutions in the presence of polymer (PVP). Both the dispersed $Mn_{1-x}PS_3(SP)_{2x}$ nanoparticles and the film reversibly display fast colouration and bleaching processes upon UV and visible irradiation, respectively. The thermal relaxation of the merocyanine form (in the dark) appears to be considerably hindered by intercalation.

Keywords: $MnPS_3$; Nanoparticles; Intercalate; Photochromic; Spiropyran

1. Introduction

Photochromic materials are of great interest due to their applications in ophthalmic lenses, communication systems, optical storage and memory devices [1–4]. Photochromism in spiropyrans involves photo-cleavage of the C–O bond, which allows reversible switching between a colourless closed form (SP) and a strongly coloured open merocyanine form (MC) [1–5], as shown in Scheme 1. In order to render the photochromic effect useful for solid state applications, the active molecules must be embedded in a solid matrix, since photochromic species in their pure crystalline form are usually inactive [1]. Classical strategies include dispersion of the molecular species in organic polymers [6–9] and organogel [10], in silica or related inorganic gels [11,12], in hybrid inorganic–organic composites such as mesoporous silicates and layered intercalation compounds [13–17].

In the search for new multifunctional materials, some of us found that photo responsive organic ions could be intercalated in layered $MnPS_3$, affording hybrid intercalates that possessed various "combined" properties [18–26]. However, the practical applications of intercalation materials are rather limited because many of them are usually available only in powders. To be appropriate in optical devices for further potential applications, these materials must be easy to process and possess good transparency. The nanoscale material should meet this requirement because the small particles are possibly dispersed in the transparent medium or generate thin film which has the high quality transparency for special photonic devices. Further potential interest in the search for such hybrid nanosystems also arose from the recent result, that dispersable nanoparticles (10 nm) consisting of specific hyperpolarizable stilbazolium chromophores inserted in $MnPS_3$ could be synthesized and afforded giant quadratic optical nonlinearity (β) [27]. When photochromic *N*-methylated pyridospiropyran cations were used in the bulk materials of hybrid $MnPS_3$, intercalation considerably stabilized the merocyanine form, to such an extent that the MC form was no longer able to revert back to the spiropyran form in the absence of prolonged irradiation by visible light. Such a dramatic stabilization was ascribed to the formation of *J*-aggregates by the MC planar forms within the weakly polar interlayer medium [26]. Merging the above features of photochromism, nanoparticles and *J*-aggregates, the challenging idea comes up that if the peculiar photochromic behavior of the spiropyran–$MnPS_3$ compounds

* Corresponding author. Fax: +86 21 55664621.
** Corresponding author. Fax: +33 1 69154754.
E-mail addresses: yitao@fudan.edu.cn (T. Yi), rclement@icmo.u-psud.fr (R. Clement).

1010-6030/$ – see front matter © 2006 Elsevier B.V. All rights reserved.
doi:10.1016/j.jphotochem.2006.08.005

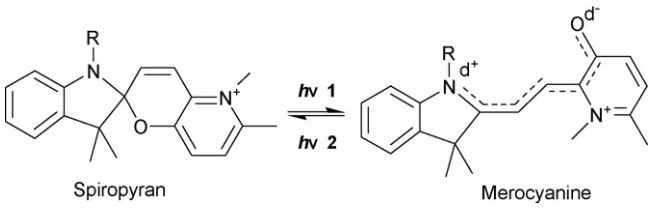

Scheme 1. Photochromism in spiropyran.

could be "transposed" to the nanometer scale, not only would the theoretical data storage capacity be increased, but very sensitive and efficient nanosystems might be designed if simultaneous or cooperative switching of all chromophores within a single nanoparticle could be achieved. In this report, we used *N*-methylpyridospiropyran (R = Me, see Scheme 1) as the photochromic guest to obtain photo responsive $Mn_{1-x}PS_3(SP)_x$ nanoparticles along a "bottom-up" synthesis. Moreover, the transparent thin film possible for fabricating devices was also achieved.

2. Experimental

2.1. Reactants

Chemicals were used as received. Brij-97 {polyoxyethylene(10)oleyl ether, $C_{18}H_{35}(OCH_2–CH_2)_nOH$, $n \sim 10$, FW: 709.00} was purchased from Sigma–Aldrich, Manganese(II) chloride (99%), cyclohexane (>99.5%), PVP (polyvinylpyrrolidone, MW 10,000, >95%), PCl_3, and sodium sulfide were purchased from Sinopharm Chemical Reagent Co. Ltd. *N*-Methylpyridospiropyran iodide (SP^+I^-) was prepared according to a previous method [4]. $Na_4P_2S_6{\cdot}6H_2O$ was obtained by dropwise addition of PCl_3 (10 mL) to aqueous solution of Na_2S (120 g/120 mL) at 5 °C under vigorous stirring [28]. The raw solid was filtered and recrystallized from hot water, yield 2.3 g (50%).

2.2. Methods and techniques

Infrared spectra of powders were obtained at room temperature on an IR PRESTIGE-21 spectrometer using KBr pellets. UV visible spectra were obtained with a Shimadzu 2550 spectrometer (Japan). Transmission electron microscopy (TEM) was recorded by JEOL JEM 2011 (Japan) operated at 200 kV attached with an energy dispersive X-ray analysis. Samples were prepared by evaporating a drop of solution on a carbon (Agar) grid. Shimadzu SSX-550 (Japan) was used for scanning electron microscopy (SEM) study. Irradiations were carried out on both dispersed colloid sample and thin films using a CHF-XM550W power system (China). Visible light was generated by a 500 W Xe lamp with a standard band-pass filter 550 AF10 (Omega). Irradiations in the UV region were effected at 365 nm. Irradiations of the films were carried out directly inside the sample holder.

2.3. Synthesis of the hybrid

$Mn_{1-x}PS_3(SP)_{2x}$ (abbreviated as: SP–$MnPS_3$) nanoparticles were carried out by a modified method according to our recently published procedure [27]. Microemulsion was achieved by using inverse, water containing micelles dispersed in cyclohexane in the presence of the Brij-97 surfactant (polyoxyethlene-oleyl ether(10), concentration of 0.8 g/10 mL). In a typical experiment, two micelle solutions (20 mL organic phase, respectively) were prepared separately, one of them containing 0.6 mL of an aqueous solution of $MnCl_2$ (9.9 mg) and 10 mg of LiCl, the other one containing an aqueous solution of $Na_4P_2S_6$ (12.8 mg in 0.6 mL H_2O). When the two systems were mixed under vigorous stirring, pale coloured micelles formed within a few minutes. At this stage 1 mL of a solution of SP^+I^- (6.6 mg) in water/methanol (2:1 v/v) was added to the mixture and stirred for 1 h avoiding daylight. The emulsion was subsequently broken by adding ethanol, yielding pale pink powder isolated by centrifugation, then washed with methanol to remove the surfactant. Elemental analysis indicated that the N/C ratio as well as the N/Mn ratio were very close to the values expected from the parent bulk compound [26]. Calc. for $Mn_{0.89}PS_3(SP)_{0.22}(H_2O)_4(LiCl)_2$, C, 13.19; H, 3.29; N, 1.54; S, 24.02; Mn, 12.21; Found: C, 13.38; H, 2.98; N, 1.57; S, 21.32; Mn, 12.30.

3. Results and discussion

3.1. Synthesis

In the present modified process, a mixture of $MnCl_2$ and LiCl was employed instead of $MnCl_2$ only. From a long experience, the presence of alkali ions often favors ionic exchange in the MPS_3 family [29]. Indeed, adding LiCl turned out to have a dramatic effect, as the powder collected was much close to the expected component from the element analysis and IR spectra (Fig. 1), even though an amount of water still existed. The powder collected did not show sharp XRD diffraction peaks, only a very broad band with a distance around 14 Å was visible. This is typical of ultra small crystalline corresponding to interlayer distances for SP–$MnPS_3$ intercalate [26]. Finally, the powder collected could be easily redispersed in water or some organic media such as chloroform or methanol in the presence

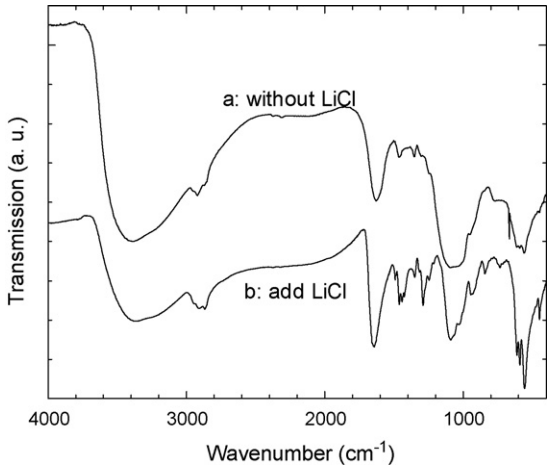

Fig. 1. Infrared spectra of (a) SP–$MnPS_3$ without LiCl and (b) SP–$MnPS_3$ with LiCl.

of polyvinylpyrrolidone (PVP, 20 mg/mL). Compared with previous method [26,29], in which achievement of the intercalate needed several ion-exchanges, the present one-pot process is much more convenient. Furthermore, due to the low solubility of hybrid MPS_3 in any solvents as well as in water, the intercalated materials from traditional method could be only obtained as a sedimentation from aqueous medium and difficult to be redispersed. Even though fine powders of Li^+ intercalated $MnPS_3$ can be suspended in water to some extent, the process is random and unquantitive. The nanoparticles from present process can be quantitively 'redissolved' in several organic mediums as well as in the polymer. This property is very convenient in view of fabrication of nanofilm or even devices.

3.2. IR spectra

The IR spectrum of the powder collected from slurry both with and without LiCl revealed four sets of bands: (a) a medium band consisting of three components (612, 591, 557 cm^{-1}), very similar to the band that appears in the same wavenumber region in the *crystalline parent* compound $Mn_{0.89}PS_3(SP)_{0.22}$ [30]. This "splitted" band is the signature intercalated MPS_3 systems and it has been assigned to the $\nu(PS_3)$ asymmetric stretching band. The $\nu(PS_3)$ band actually appears as a degenerate single band at 570 cm^{-1} in pristine MPS_3, the degeneracy being lifted upon intercalation as a consequence of the occurrence of intralamellar M^{2+} vacancies that renders the P–S bonds inequivalent [31]. (b) A series of bands between 1500 and 900 cm^{-1} as well as a broader one around 2800–2900 cm^{-1} which are readily attributed to the spiropyran species [26]. The data (a) + (b) suggest that the powder contains SP species intercalated in $MnPS_3$. (c) The broad band between 1150 and 1000 cm^{-1} undoubtedly reveals the presence of an amount of "phosphate species" whose formation is due to the hydrolysis of a fraction of the fragile $(P_2S_6)^{4-}$ anions. (d) Two bands (3400 cm^{-1} very broad, 1600 cm^{-1} sharp) show the presence of an amount of water retained in the powder. The IR spectrum of the improved powder (Fig. 1b, with LiCl) readily showed that the $\nu(PS_3)$ components around 570 cm^{-1} dominated over the phosphate band around 1100 cm^{-1}. In addition, the sharp bands between 1500 and 950 cm^{-1}, assigned to spiropyran, were also much stronger. Therefore, the IR data indicate that the improved powder contained much more of the seeked intercalate.

3.3. Morphology of the nanoparticles

The morphology of the nanoparticles were investigated by TEM. A typical TEM image after evaporating a drop of a water dispersion of the particles on a grid is shown in Fig. 2a. The images display a rather homogeneous distribution of nanoparticles of about 10–20 nm in size. These particles trend to be agglomerated in hyperbranched structures. The formation of a hyperbranched structure is associated with the wire like "head-to-tail" alignment of the particles. Whereas in methanolic dispersion, the particles tend to form two dimensional larger conglomerate as shown in Fig. 2b. EDX analysis of all these samples yielded the expected Mn, P, S stoichiometry. The SEM image of a film obtained by spreading a methanol/PVP solution on a glass plate shows a pattern of conglomerates quite uniform in size, around 200 nm (Fig. 2c).

3.4. Photochromic properties of the nanoparticles

The photochromic properties of the nanoparticles were characterized by absorption spectra. Prior to any irradiation, the colloid formed by the SP–$MnPS_3$ nanoparticles dispersed in PVP/chloroform (20 mg PVP/mL chloroform, the concentration of SP in colloid is 2.8×10^{-4} mol/L) was pale yellow, and its spectrum showed no band above 350 nm, clearly indicating that the guest species were under their SP (close) forms. Upon irradiation at 365 nm for 10 min, the colloid rapidly turned to violet. A new band peaking around 560 nm ($\varepsilon_{particle} = 1.3 \times 10^3\ M^{-1}\ cm^{-1}$) grew, characteristic of the MC (open) form. Irradiation by visible light at 550 nm caused a rapid decay of the absorption band, hence the MC form turned back to SP form easily (Fig. 3).

A solid film was prepared by spreading the PVP/chloroform solution of the colloidal particles on a glass plate and drying it up. Irradiation at 365 nm caused the film to turn to violet, because of the growth of the 560 nm band. Bleaching occurred very rapidly upon irradiation by visible 550 nm light (Fig. 4a). Nevertheless colouration as well as bleaching proceeded significantly slower in the film than in the colloid, as shown in Fig. 4a, the difference

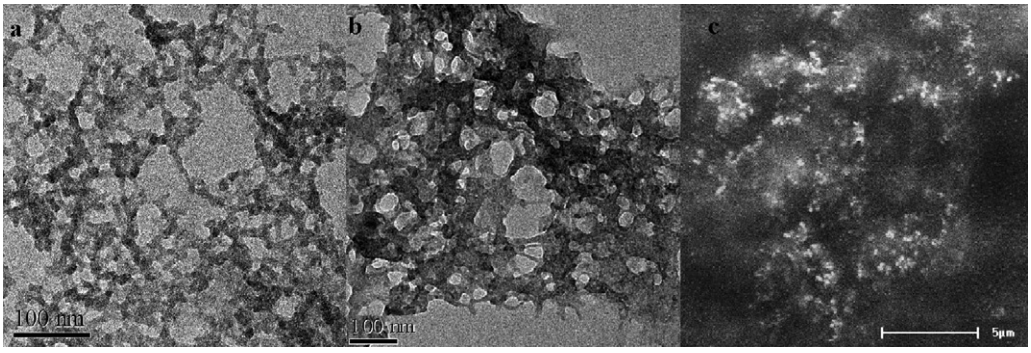

Fig. 2. TEM images of SP–$MnPS_3$ nanoparticles dispersed in water (a) and methanol (b); SEM images of SP–$MnPS_3$ nanofilm on PVP (c).

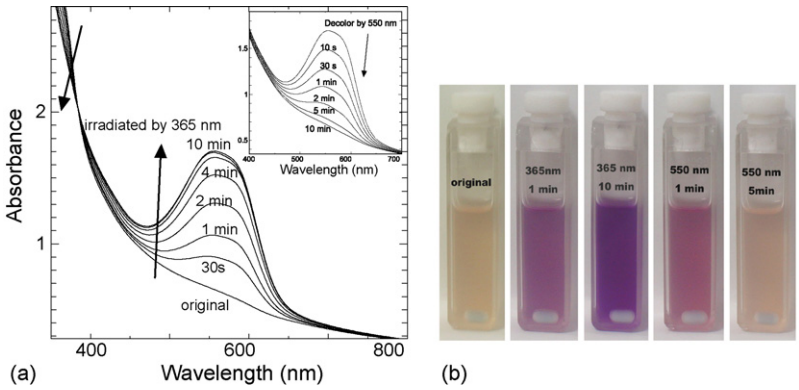

Fig. 3. (a) The absorption spectral changes of dispersed SP–$MnPS_3$ nanoparticles upon UV irradiation (365 nm, 0.26 mW/cm^2, $[c]_{SP} = 2.8 \times 10^{-4}$ mol/L). The inset shows the spectral changes of the irradiated sample upon visible bleaching (550 nm, 38.9 mW/cm^2). (b) Photographs of the sequential process of colour generation and bleaching for dispersed SP–$MnPS_3$ nanoparticles.

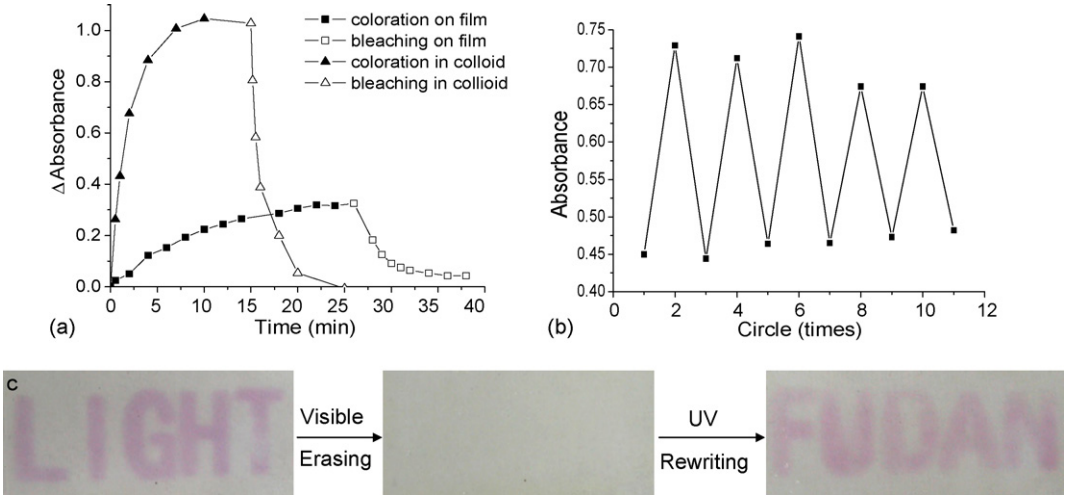

Fig. 4. (a) Time dependence of the absorption at 550 nm of dispersed SP–$MnPS_3$ nanoparticles (triangle mark, $[c]_{SP} = 2.0 \times 10^{-4}$ mol/L) and of nanofilm (square mark), respectively, under irradiation (365 nm, filled mark) and bleaching (550 nm, empty mark). (b) Cycles of colouration and bleaching on the nanofilm. (c) Photo-rewritable imaging on the nanofilm of SP–$MnPS_3$ by using UV (365 nm, hand-held lamp) and visible light (>500 nm). The violet regions represent the parts irradiated with UV light.

being more pronounced for colouration than for bleaching. Thus, for colouration, ν_0(film) equals 0.13 min^{-1}, about three times smaller than ν_0(colloid) (0.32 min^{-1}). The photo bleaching rate constants at the early stage for film, k_0(film) = 0.22 min^{-1}, is also smaller than that for colloid, k_0(colloid) = 0.87 min^{-1}. The result suggests that the visible light induced bleaching rate is comparable with that of colouration process in the nanosystem. While in the solid state, the bleaching rate was about 200 times slower than that of colouration because of the formation of the *J*-aggregate [26]. The colouration and bleaching of the nanofilms can undergo several cycles (Fig. 4b).

3.5. Thermal relaxation of the merocyanin–$MnPS_3$ nanoparticles

The kinetics of the relaxation in the dark of both the MC–$MnPS_3$ colloid and film were followed by monitoring the decay of the absorbance at 550 nm as a function of time. Results were compared with the relaxation of photostationary "free" MC iodide in chloroform solution (Fig. 5). The

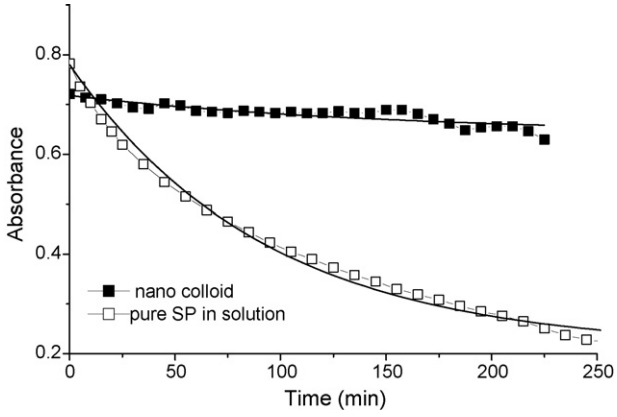

Fig. 5. Comparison of the relaxation in the dark of MC–$MnPS_3$ nanoparticles and of free merocyanine iodide. The figure plots the time dependence of the absorption at 550 nm of dispersed nanoparticles (colloid, $[c]_{SP} = 1.4 \times 10^{-4}$ mol/L) and of a solution of free SP iodide after they have reached the photostationary state (1.4×10^{-4} mol/L in chloroform) in the dark. The plots were fitted by first-order equations.

curves afforded by the colloid and by "free" solution were fitted by first-order laws [32] giving $k_{\text{colloid}} = 9.3 \times 10^{-4}\ \text{min}^{-1}$ and $k_{\text{free solution}} = 9.1 \times 10^{-3}\ \text{min}^{-1}$, respectively. The decay of the MC–$MnPS_3$ nanoparticles synthesized in this work is therefore about 10 times slower than the decay of "free" molecular MC species in solution. Typically, half of the MC–$MnPS_3$ nanoparticles stored in the dark switched back to SP over 1 day, but at this point we can not say whether all MCs in a given particle switch in a correlated manner or not. We only note here that the unexpected rapid bleaching of the film deserves further investigation, because it might be related to some collective behavior of the chromophores.

Therefore, the photochromic properties of the SP–$MnPS_3$ nanoparticles under UV irradiation are markedly different from those of the parent bulk intercalate, in which the colour eventually turned to blue, beyond the violet stage which was only an intermediate. That blue state, extremely stable, has been suggested to be a *J*-aggregated state of the planar merocyanine forms [26]. It is obvious that irradiation of the present hybrid SP–$MnPS_3$ nanoparticles does not lead to *J*-aggregate state, a difference that may be due to surface disorder effects, poor packing of the SP chromophores and/or poor crystallization of the nanoparticles. Nevertheless this work clearly shows that intercalation of the SP species results in a dramatic hindrance of the thermal relaxation of the merocyanine forms, which is probably due to the strong ionic packing forces between the negatively charged host lattice and the positively charged SP species. Moreover, the obviously quick responsibility on both photo irradiation and photo bleaching in the present nanosystem comparing with the parent bulk intercalate, is of importance for practicability. In addition, the practical capability of rewritable photoimaging on our nanofilm was investigated by patterned illumination through photomasks. The word 'LIGHT' was recorded as a first image (Fig. 4c), which was subsequently erased and followed by the recording of a second image, the name of our university (FUDAN). This successful demonstration of rewritable photoimage suggests the potential application of hybrid SP–$MnPS_3$ nanoparticles to rewritable optical memory media or imaging processes.

4. Conclusions

In conclusion, this report brings about a significant step towards the achievement of air-stable, nanometer-size objects exhibiting reversible photochromism. In particular, the thermal relaxation of the nanocolloid is dramatically hindered as compared to the free chromophores. It may be conjectured that further improvements of the system might thus lead to fully bistable nanoparticles having no thermal relaxation at all, which could constitute interesting nanomemories.

Acknowledgements

This work was supported by National Science Foundation of China (NSFC 20441006 and 20571016).

References

[1] J.C. Crano, R.J. Guglielmetti, Organic Photochromic and Thermochromic Compounds, Plenum Press, New York, 1999.
[2] B.L. Feringa, W.F. Jager, B. de Lange, Tetrahedron 49 (1993) 8267.
[3] W. Yuan, L. Sun, H. Tang, Y. Wen, G. Jiang, W. Huang, L. Jiang, Y. Song, H. Tian, D. Zhu, Adv. Mater. 17 (2005) 156.
[4] S. Bénard, P. Yu, Adv. Mater. 12 (2000) 48.
[5] X. Guo, Y. Zhou, D. Zhang, B. Yin, Z. Liu, C. Liu, Z. Lu, Y. Huang, D. Zhu, J. Org. Chem. 69 (2004) 8924.
[6] M. Levitus, M. Talhavini, R. Martin Negri, T.D.Z. Atvars, P.F. Aramendia, J. Phys. Chem. B 101 (1997) 7680.
[7] M. Levitus, P.F. Aramendia, J. Phys. Chem. B 103 (1999) 1864.
[8] G. Berkovic, V. Krongauz, V. Weiss, Chem. Rev. 100 (2000) 1741.
[9] X. Guo, D. Zhang, G. Yu, M. Wan, J. Li, Y. Liu, D. Zhu, Adv. Mater. 16 (2004) 636.
[10] A. Shumburo, M.C. Biewer, Chem. Mater. 14 (2002) 3745.
[11] D. Levy, D. Avnir, J. Phys. Chem. 92 (1988) 4734.
[12] R.A. Evans, T.L. Hanley, M.A. Skidmore, T.P. Davis, G.K. Such, L.H. Yee, G.E. Ball, D.A. Lewis, Nat. Mater. 4 (2005) 249.
[13] J. Biteau, F. Chaput, J.P. Boilot, J. Phys. Chem. 100 (1996) 9024.
[14] S. Benard, E. Rivière, P. Yu, K. Nakatani, J.F. Delouis, Chem. Mater. 13 (2001) 159.
[15] B. Schaudel, C. Guermeur, C. Sanchez, K. Nakatani, J.A. Delaire, J. Mater. Chem. 7 (1997) 61.
[16] G. Wirnsberger, B.J. Scott, B.F. Chmelka, G.D. Stucky, Adv. Mater. 12 (2000) 1450.
[17] N. Andersson, P. Alberius, J. Örtegren, M. Lindgren, L. Bergström, J. Mater. Chem. 15 (2005) 3507.
[18] B.I. Ipe, S. Mahima, K.G. Thomas, J. Am. Chem. Soc. 125 (2003) 7174.
[19] P.G. Lacroix, K. Nakatani, Adv. Mater. 9 (1997) 1105.
[20] P.G. Lacroix, R. Clément, K. Nakatani, J. Zyss, I. Ledoux, Science 263 (1994) 658.
[21] R. Clément, P.G. Lacroix, J.S.O. Evans, D. O'Hare, Adv. Mater. 6 (1994) 794.
[22] R. Clément, Hybrid organic–inorganic composites, in: J.E. Mark, Y.C. Lee, P. Bianconi (Eds.), Proceedings of the ACS Symposium Series 585, American Chemical Society, Washington, DC, 1995.
[23] T. Coradin, R. Clément, P.G. Lacroix, K. Nakatani, Chem. Mater. 8 (1996) 2153.
[24] P.G. Lacroix, I. Malfant, S. Bénard, P. Yu, E. Rivière, K. Nakatani, Chem. Mater. 13 (2001) 441.
[25] S. Bénard, P. Yu, J.P. Audière, R. Clément, J. Guilhem, L. Tchertanov, K. Nakatani, J. Am. Chem. Soc. 122 (2000) 9444.
[26] S. Benard, A. Leaustic, E. Rivière, P. Yu, R. Clement, Chem. Mater. 13 (2001) 3709.
[27] T. Yi, N. Tancrez, R. Clement, I. Ledoux-Rak, J. Zyss, Adv. Mater. 17 (2005) 335.
[28] H. Falius, Z. Anorg. Allg. Chem. 356 (1968) 189.
[29] I. Lagadic, P.G. Lacroix, R. Clement, Chem. Mater. 9 (1997) 2004–2012.
[30] R. Clement, O. Garnier, J. Jegoudez, Inorg. Chem. 25 (1986) 1409.
[31] U. Albrecht, H. Schäfer, R. Richert, Chem. Phys. 182 (1994) 61.
[32] T. Yi, K. Sada, K. Sugiyasu, T. Hatano, S. Shinkai, Chem. Commun. 3 (2003) 344.